ELSEVIER

PII: S0032-3861(97)00215-2

Polymer Vol. 38 No. 26, pp. 6371–6378, 1997

0032-3861/97/$17.00+0.00

Compatibility and properties of alternating ethylene–tetrafluoroethylene copolymer and poly(methyl methacrylate) blends

Jiyun Feng and Chi-Ming Chan*
Department of Chemical Engineering, The Hong Kong University of Science and Technology, Clear Water Bay, Kowloon, Hong Kong
(Received 21 October 1996; revised 23 December 1996)

Blends of an alternating ethylene–tetrafluorethylene copolymer (ETFE) and poly(methyl methacrylate) (PMMA) were prepared by melt mixing in a mixer. Compatibility, thermal behaviour and morphology of the blends of various compositions were investigated by using dynamic mechanical analysis (d.m.a.), Fourier transform infra-red spectroscopy (*FT*i.r.), solid-state nuclear magnetic resonance (n.m.r.) spectroscopy, differential scanning calorimetry (d.s.c.) and wide-angle X-ray diffraction. D.m.a. and d.s.c. results show that the glass transition temperature (T_g) of the ETFE in the blends increases as the PMMA content increases and the T_g of the PMMA moves to low temperatures when the ETFE content increases. In addition, d.s.c. results indicate an additional T_g, which is located between the T_g of PMMA and that of ETFE. The presence of this additional T_g suggests the existence of one semicrystalline phase and two amorphous phases—an ETFE/PMMA phase and a PMMA-rich phase. D.s.c. results also indicate that the melting temperature of ETFE decreases while the crystallinity of ETFE increases slightly as the PMMA content increases. *FT*i.r. results show that the absorption peak of the carbonyl group of the PMMA in the blends stays almost at the same position as in the pure component. Solid-state n.m.r. results reveal that the changes in chemical shift of the carbonyl group of PMMA in the blends are less than 0.5 ppm. These results confirm that only weak interactions exist between ETFE and PMMA. X-ray diffraction results reveal that no new crystal forms appear in the blends. © 1997 Elsevier Science Ltd.

(Keywords: ETFE; PVF_2; blends; compatibility)

INTRODUCTION

Compatibility of polymers has been one of the important areas in the field of polymer science during the last two decades[1–15]. One of the most extensively studied polymer blend systems is poly(vinylidene fluoride) (PVF_2) and poly(methyl methacrylate) (PMMA). PVF_2 and PMMA are compatible polymers in the melt. At temperatures at which PVF_2 crystallizes, phase separation occurs and the blend is then regarded as a semicompatible system comprising a semicrystalline phase and an amorphous phase[16]. The compatibility of these blends is attributed to the negative value of the Flory–Huggins parameter owing to the specific interaction involved between the CH_2 group of PVF_2 and the carbonyl group of PMMA[17]. There are many other studies on the blends of PVF_2 with other polymers[18–24]; however, there are very few studies on the blends of PMMA with other fluoropolymers. An ethylene–tetrafluoroethylene copolymer (ETFE) is an isomer of PVF_2. ETFE has been used commercially in various high-performance products, but only a few studies have been made on its physical properties[25–29]. Studies of the blends of ETFE with other polymers are absent in the literature. On the basis of the solubility parameter concept, ETFE and PVF_2 have very similar solubility parameters. It appears to be natural to study the blends of ETFE and PMMA because this study would allow us to determine the dependence of the interaction parameter on chemical structure.

In this work, we shall focus our study on the compatibility and morphology of the ETFE/PMMA blends. The techniques employed included dynamic mechanical analysis (d.m.a.), Fourier transform infra-red spectroscopy (*FT*i.r.), solid-state nuclear magnetic resonance (n.m.r.) spectroscopy, differential scanning calorimetry (d.s.c.) and wide-angle X-ray diffraction (WAXD).

EXPERIMENTAL

The ETFE used in this study is an alternating ethylene–tetrafluorethylene copolymer supplied by Du Pont, USA. The PMMA was purchased from Scientific Polymer Products Co., Canada. The inherent viscosity of the PMMA is 0.45. ETFE/PMMA blends were prepared with a Haake Rheocord mixer 9000 at 280°C for 10 min. Sheets of thickness of about 1.5 mm were prepared by using a hot press at 250°C. The weight ratios of ETFE to PMMA in the blends were 100/0, 80/20/ 60/40, 50/50, 40/60, 20/80 and 0/100.

Dynamic mechanical measurements were performed with a dynamic mechanical analyser (TA DMA 983). The frequency was 3.5 Hz. The heating rate was 3°C min^{-1} and the temperature range was from − 120°C to 150°C. Specimen dimensions were 1.4 cm × 1.4 cm × 0.15 cm.

A Fourier transform infra-red spectrometer (Bio Rad model FTS 6000) was used to study the interactions between ETFE and PMMA. The reflection mode was used and the reflection angle was 60°. All spectra were recorded at ambient temperature and a minimum of 128 scans were

* To whom correspondence should be addressed

obtained. The signals were averaged with a resolution of 2 cm^{-1}.

Cross-polarization/magic-angle spinning (CP/MAS) ^{13}C n.m.r. spectra of the ETFE/PMMA blends were measured at room temperature on a JEOL EX-400 NMR spectrometer. Samples were spun at 5.0–5.3 kHz in a 6 mm rotor. A cross-polarization pulse was used with a contact time of 2.0 ms.

The study on the crystallization and melting behaviour of the ETFE/PMMA blends was performed with a differential scanning calorimeter (TA 2100). The instrument was calibrated with indium as a standard and all measurements were conducted under a nitrogen atmosphere. Sample weights of 10 to 12 mg were used. All samples were first heated to 300°C to remove the prior thermal histories. Then they were cooled to room temperature at a cooling rate of 20°C min^{-1} to observe the cooling crystallization process, followed by heating the samples to 300°C again at a heating rate of 20°C min^{-1} to observe the melting behaviour. The heats of crystallization and fusion were calculated from the areas of the crystallization and melting peaks, respectively. The endotherm and exotherm peaks were taken as the melting temperature (T_m) and the crystallization temperature (T_c), respectively.

The WAXD patterns of the ETFE/PMMA blends were obtained with a Philips PW 1830 diffractometer equipped with Cu K_α radiation operating at 40 kV and 50 mA at room temperature. The angular scale and recorder reading (2θ) were calibrated to an accuracy of 0.01°. The diffraction angle varied from 3° to 35°. Samples for the X-ray measurements were of uniform thickness of 1.5 mm.

RESULTS AND DISCUSSION

Compatibility

D.m.a. results. D.m.a. is a sensitive and powerful tool to assess the compatibility of polymer blends. *Figure 1* shows the storage modulus of the ETFE/PMMA blends as a function of temperature. As the temperature increases the storage modulus decreases. A sharp decrease is observed for PMMA and the blends at the glass transition temperature (T_g) of PMMA, and this is attributed to an increase in the segment mobility of PMMA as the temperature increases. For the pure ETFE, there is also a sharp decrease observed in log E' at approximately 70°C, which may be regarded as the glass transition of ETFE. Controversy still exists over the exact position of the glass transition temperature of a number of fluoropolymers such as polytetrafluoroethylene and poly(vinylidene fluoride)[30] because of the existence of several transitions. It should be noted that as the PMMA content increases, the modulus of the blends also increases. The higher modulus of the blends is caused by the high modulus of PMMA.

The loss modulus and tan δ of the blends as a function of temperature are shown in *Figures 2 and 3*, respectively. The

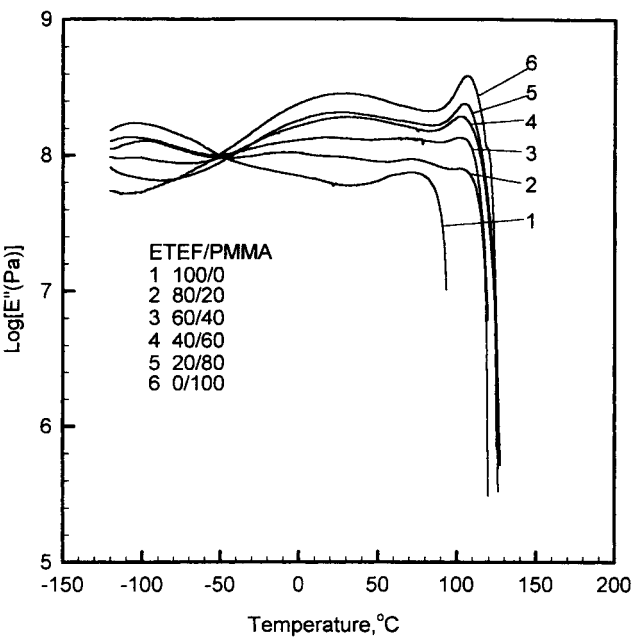

Figure 2 Loss modulus, E'' *versus* temperature for the ETFE/PMMA blends

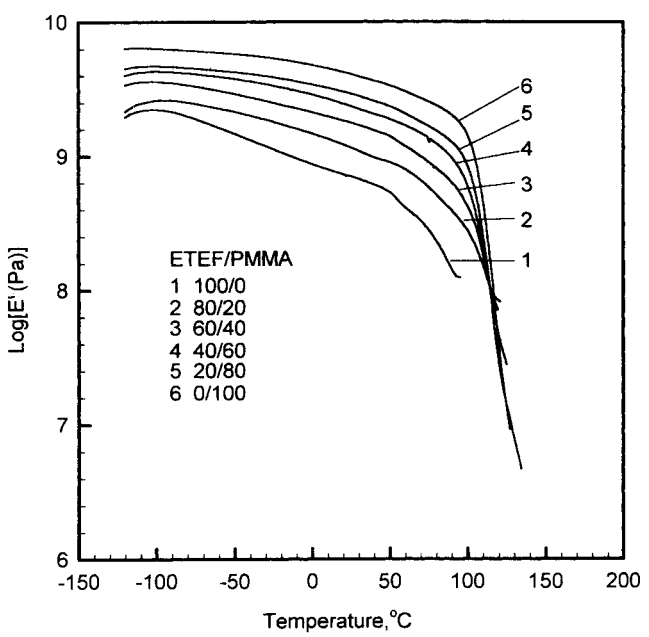

Figure 1 Storage modulus, E' *versus* temperature for the ETFE/PMMA blends

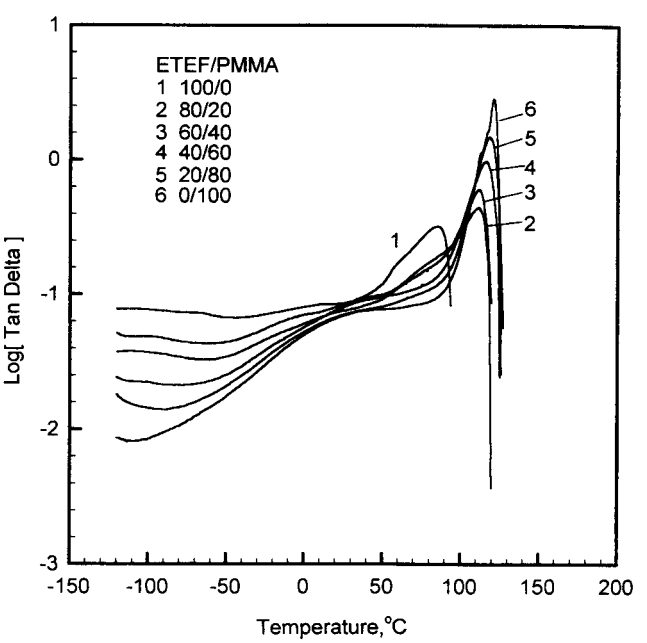

Figure 3 Tan δ *versus* temperature for the ETFE/PMMA blends

loss modulus peak at 106.9°C for PMMA is commonly identified as the glass transition temperature for this polymer. However, the location of the T_g for ETFE is more problematic. At first sight, the loss modulus peak at 71.8°C would be a reasonable guess for the glass transition temperature for ETFE. However, a close examination of the tan δ curve for ETFE, as shown in *Figure 4*, reveals that there are four transitions: α, β, γ and δ transitions at approximately 84, 13.4, -68 and -110°C, respectively. The T_gs of PMMA and ETFE in the blends, as determined by using the loss modulus, is shown in *Figure 5*. For the blends, the two relaxation peaks (the α-relaxation peak of ETFE and glass transition temperature of PMMA) are observed when the ETFE content is high. It is noted that the T_g of PMMA in the blends shifts to low temperatures as the ETFE content increases, while the change in T_g of ETFE is difficult to detect at high PMMA contents because of the broad β-relaxation peak of PMMA. The shifting of the α-relaxation peak of ETFE as a function of blend composition may provide some support to the assignment of the α-relaxation peak as the glass transition temperature of ETFE.

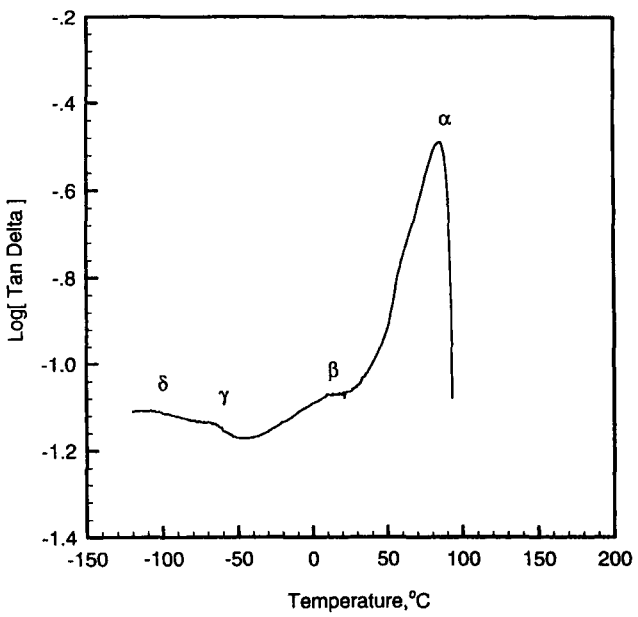

Figure 4 Tan δ *versus* temperature for pure ETFE

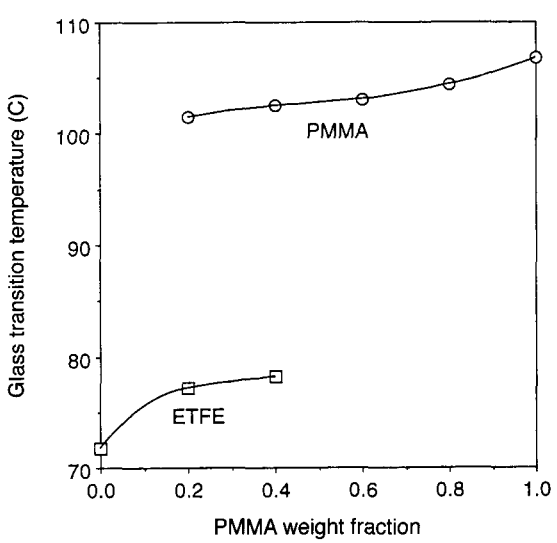

Figure 5 T_gs of the blends determined from E'' data

D.s.c. results. The miscibility of polymer blends is most commonly defined by the presence of a single glass transition temperature as observed in d.s.c. scans. *Figure 6* shows the d.s.c. curves of the slowly cooled ETFE/PMMA blends of various compositions. It is apparent that at least two T_gs are observed, indicating that these polymers are not miscible. The low and high T_gs correspond to the glass transition temperature of ETFE and PMMA, respectively. The plot of T_g as a function of blend composition is shown in *Figure 7*. It is found that the low T_g shifts slightly to high temperatures as the PMMA content increases and the high T_g shifts to low temperatures as the ETFE content increases. This is clear

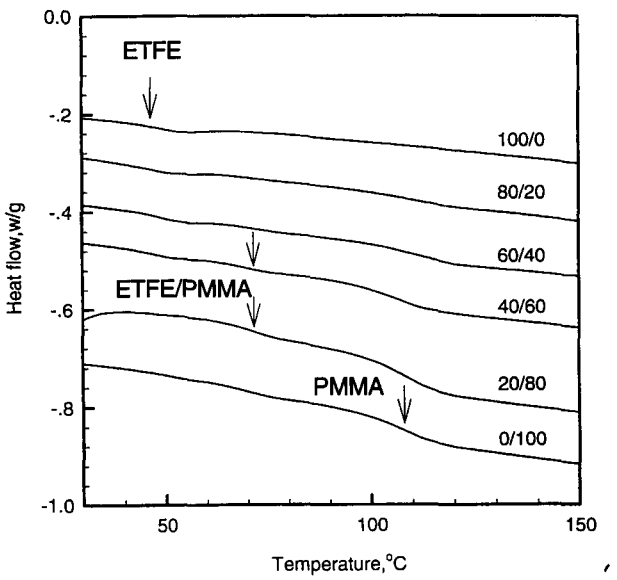

Figure 6 D.s.c. scans for the slowly cooled ETFE/PMMA blends

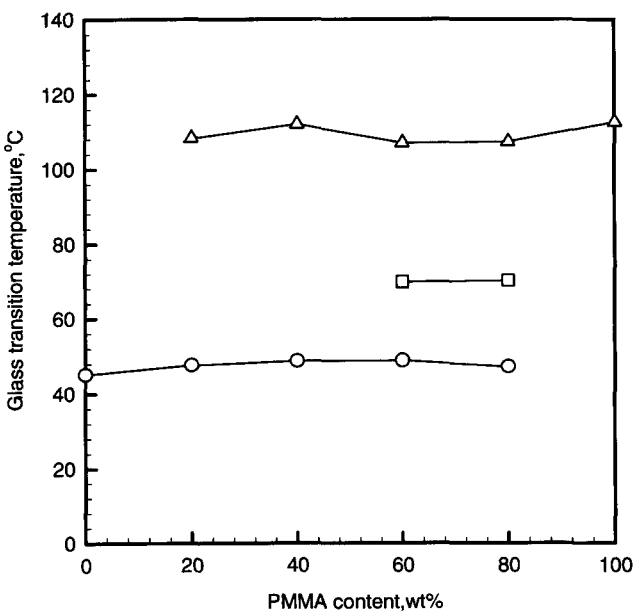

Figure 7 T_gs of the slowly cooled ETFE/PMMA blends: △, PMMA-rich phase; □, ETFE/PMMA amorphous phase; and ○, ETFE semicrystalline phase.

evidence of the fact that the ETFE/PMMA blends are semi-compatible systems that are similar to the blends of PVF_2 and PMMA. Because the extent of the T_g shift is small, the blends only have limited miscibility.

In the d.s.c. scans as shown in *Figure 6*, an additional transition can be identified when the ETFE content is lower that 40 wt%. This transition is located between the low and high T_gs but near the low T_g, as marked by the arrows. The presence of this additional T_g could be evidence of the existence of a third phase. By using the Fox equation, the weight fraction of ETFE in this phase (ETFE/PMMA phase) was estimated to be approximately 0.55. This result is consistent with the chemical composition of the ETFE/PMMA phase of the blends determined by time-of-flight secondary-ion mass spectrometry[31]. The presence of such a three-phase structure was also observed for the blends of poly(ethylene oxide) and PMMA[32].

The presence of this ETFE/PMMA amorphous phase can be enhanced by rapid quenching of the samples. Quenching treatment of a polymer sample can obviously suppress the crystallinity of the polymer and increase the amorphous content. When the samples were quenched from the melt to ice water, the T_g of the pure ETFE is measured to be at 39°C, as shown in *Figure 8*, instead of at 46°C which was measured for the slowly cooled sample. The change in the α-relaxation peak as a function of crystallinity is further evidence supporting the assignment of the α transition as the glass transition temperature for ETFE because it is well known that the T_g of a semicrystalline polymer increases with its crystallinity. The slight increase in the T_g of ETFE as the PMMA content increases is attributed to the increase in crystallinity in the ETFE phases as the PMMA content increases, as shown by the increase in the heat of fusion when the PMMA content increases (see a later section on thermal properties). For the quenched samples, the detection of this additional T_g is easier possibly because the presence of this T_g will be overshadowed by the T_g of the pure ETFE if the ETFE content is high. The position of the T_g of the ETFE/PMMA phase is relatively independent of the composition of the blends, as shown in *Figure 8*.

From the results above, it can be concluded that the blends exhibit a three-phase structure—an ETFE semi-crystalline phase, an ETFE/PMMA amorphous phase and a PMMA-rich amorphous phase.

*FT*i.r. and solid-state n.m.r. results. The results of d.s.c. and d.m.a. indicate that ETFE/PMMA blends are semi-compatible. Generally speaking, semicompatibility in polymer blends is caused by some specific interactions between the two polymer molecules. *FT*i.r. is a powerful tool to determine the nature and the extent of molecular interactions in polymer blends. Only very small shifts in the peak position of the carbonyl group are observed upon addition of ETFE. The maximum shift is less than 2 cm^{-1} and no obvious broadening of the absorption band is noted, as shown in *Figure 9*. The magnitude of the frequency shift suggests that the interactions between ETFE and PMMA are very weak. It is more likely that the specific interaction between ETFE and PMMA is between the C=O group of PMMA and the CH_2 group of ETFE[17].

Solid-state n.m.r. can also be used to detect the interactions between the two polymers. *Figure 10* displays the ^{13}C n.m.r. spectra of ETFE and PMMA. The resonance peaks at 22.31 and 118.49 ppm in the ETFE spectrum are associated with the CH_2 and CF_2 groups, respectively. The resonance peaks at 177.07, 51.75 and 44.75 ppm in the PMMA spectrum are related to the C=O group, OCH_3 group and quaternary C, respectively; and the CH_2 resonance appears as a shoulder peak on the left side of the OCH_3 resonance peak. *Figure 10* shows that the carbonyl resonance peak can be chosen to detect the change in the chemical shift caused by the interactions of the C=O and CH_2 groups. *Figure 11* shows the ^{13}C n.m.r. spectra of the ETFE/PMMA blends of various compositions and *Table 1* lists the chemical shifts of the carbonyl group. From the data shown in *Table 1*, we can see that the resonance peak of the carbonyl group shifts to higher fields as the ETFE content increases. But the changes in the chemical shift are less than 0.5 ppm. These results suggest that the interactions between ETFE and PMMA are weak and agree very well with those of *FT*i.r.

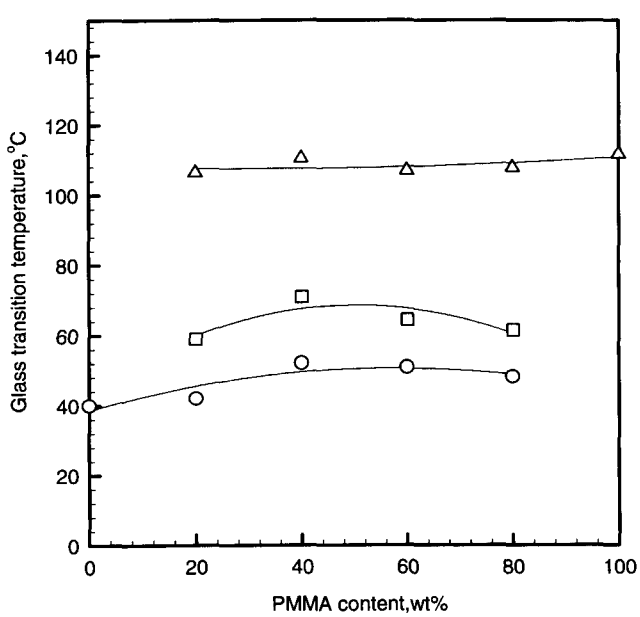

Figure 8 T_gs of the quenched ETFE/PMMA blends: △, PMMA-rich phase; □, ETFE/PMMA amorphous phase; and ○, ETFE semicrystalline phase

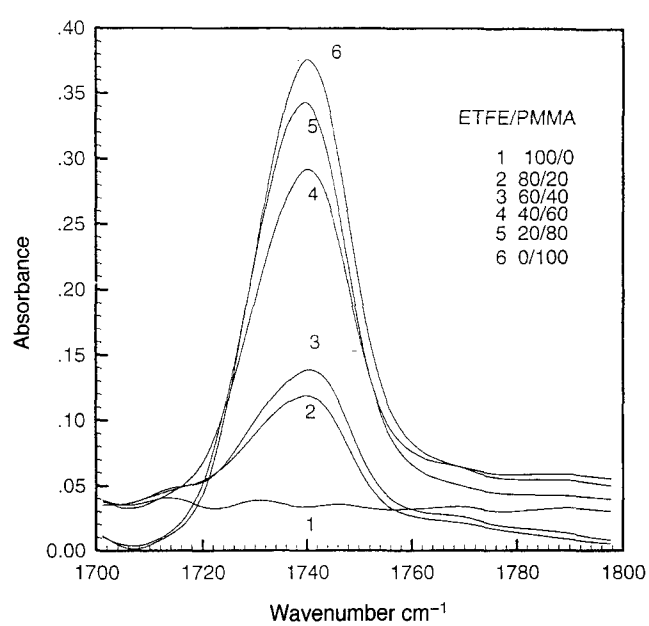

Figure 9 *FT*i.r. spectra of the ETFE/PMMA blends

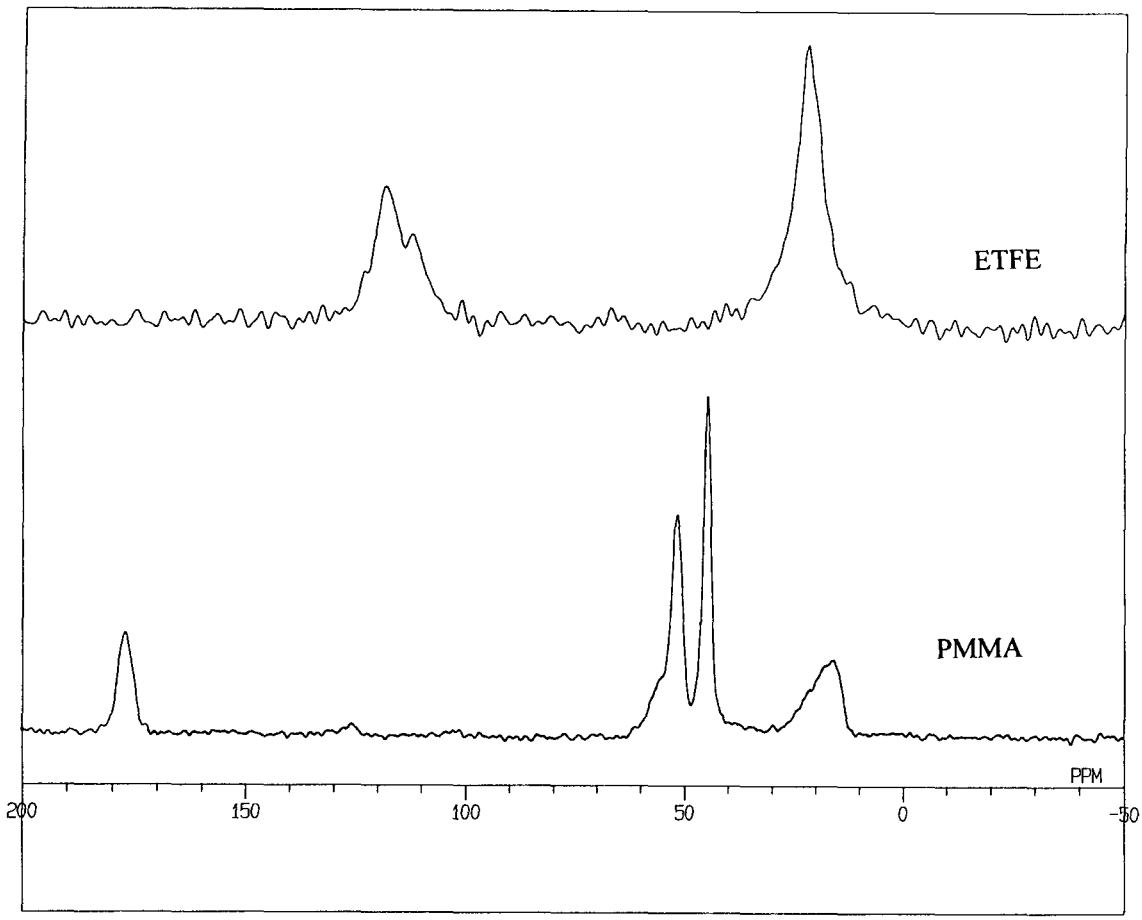

Figure 10 CP/MAS ^{13}C n.m.r. spectra of ETFE and PMMA

Thermal properties

Figure 12 shows the d.s.c. traces of the pure polymers and their blends obtained at a cooling rate of 20°C min^{-1} from 300°C. An exotherm peak at 211.4°C which is the crystallization temperature, T_c, is observed at d.s.c. cooling curves for pure ETFE and the blends. The crystallization data are listed in *Table 2*. These results suggest that the PMMA content does not affect the T_c of ETFE in the blends. However, the heat of crystallization, ΔH_c, of ETFE increases slightly as the PMMA content increases, leading to the conclusion that PMMA promotes crystallization of ETFE.

The melting behaviour of ETFE and the blends after crystallization is shown in *Figure 13*. The d.s.c. curves show a melting peak at about 240°C. The melting temperature, T_m, and the heat of fusion, ΔH_f, of pure ETFE and the blends are listed in *Table 3*. The T_m of the ETFE in the blends decreases slightly as the PMMA content increases. In fact, the shift of the T_m to low temperatures, as shown in *Figure 14*, is additional evidence that confirms that the ETFE/PMMA blends are semi-compatible. Nishi and Wang[8] derived a relationship describing the melting point depression of a crystalline polymer (component 2) owing to the presence of a miscible diluent (component 1). When the miscible diluent is a polymer, the entropy of mixing becomes negligible and the melting point depression will be largely enthalpic in nature. The resulting equation for the melting

Table 1 Chemical shifts of the carbon atom of the carbonyl group of PMMA in the blends determined by solid-state n.m.r.

ETFE/PMMA (w/w)	100/0	80/20	60/40	40/60	20/80	0/100
Chemical shift (pmm)		177.55	177.16	177.16	177.26	177.07

Table 2 Cooling crystallization data of ETFE/PMMA blends obtained by d.s.c.

ETFE/PMMA (w/w)	ΔH_c (J g^{-1})		T_c (°C)
	Blend	ETFE	
100/0	42.0	42.0	211.4
80/20	34.5	43.1	211.2
60/40	28.4	47.3	210.7
40/60	19.0	47.5	211.4
20/80	10.1	50.5	213.7

Table 3 Melting behaviour of the ETFE/PMMA blends

ETFE/PMMA (w/w)	ΔH_f (J g^{-1})		T_m (°C)
	Blend	ETFE	
100/0	46.1	46.1	240.4
80/20	41.3	51.6	239.4
60/40	31.4	52.3	239.0
40/60	21.0	52.5	237.6
20/80	10.9	54.4	234.7

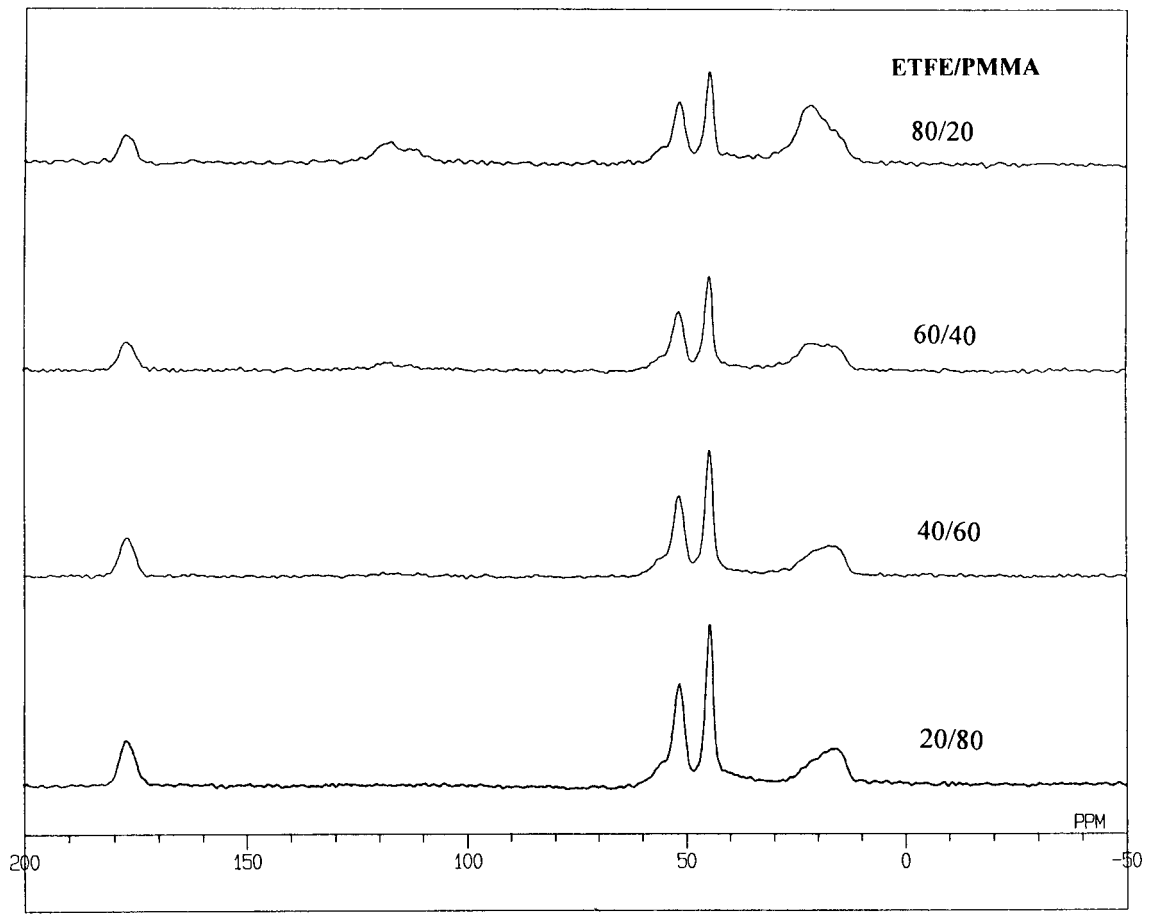

Figure 11 CP/MAS ^{13}C n.m.r. spectra of the ETFE/PMMA blends

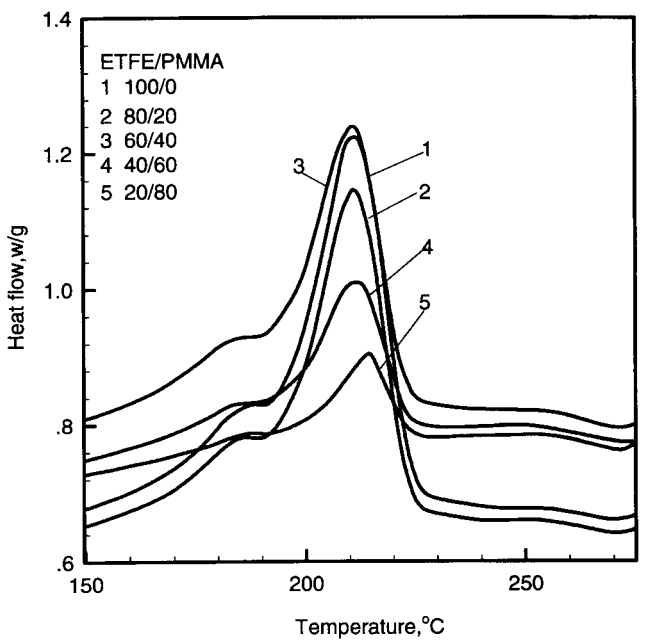

Figure 12 D.s.c. crystallization curves of the ETFE/PMMA blends obtained at a cooling rate of 20°C min^{-1}

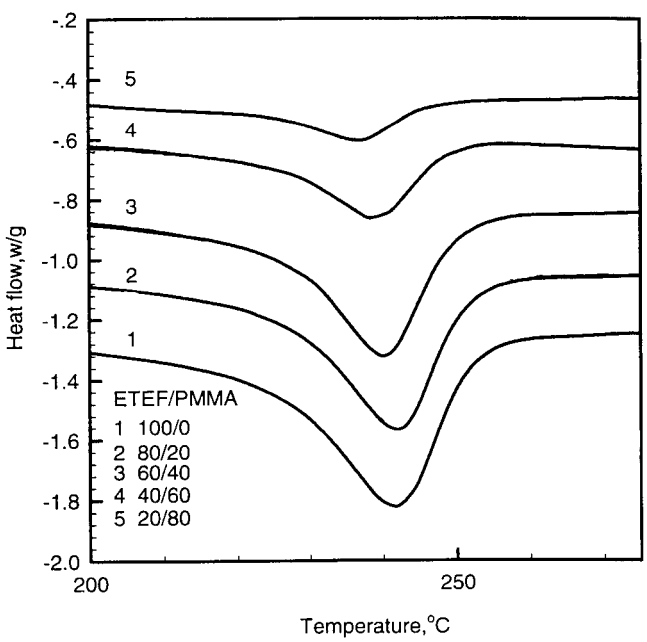

Figure 13 D.s.c. melting curves of the ETFE/PMMA blends obtained at a heating rate of 20°C min^{-1}

depression is

$$\Delta T_m = -T_m^\circ \left(\frac{V_2 B}{\Delta H_2}\right)\phi_1^2 \quad (1)$$

where ΔT_m is the equilibrium melting point depression, T_m° is the melting point of the pure crystalline polymer (component 2), V_2 and ΔH_2 are the molar volume of the repeating unit and heat of fusion per mole of repeating unit, respectively, for component 2, and ϕ_1 is the volume fraction of component 1. The term B is related to the Flory–Huggins interaction parameter χ by

$$\chi = \frac{BV_1}{RT_m} \quad (2)$$

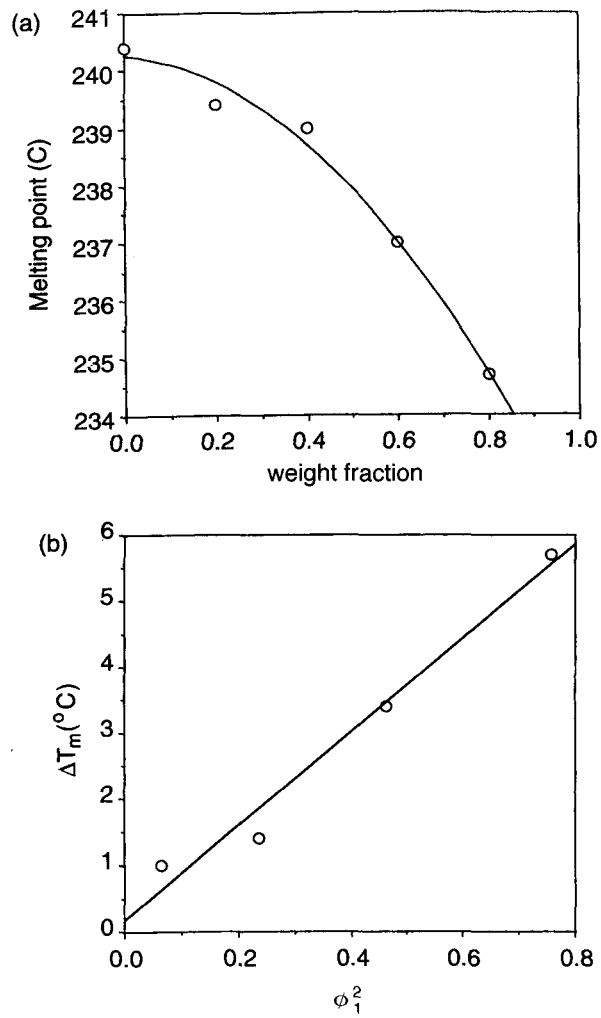

Figure 14 (a) A plot of T_m *versus* composition of the blend. (b) A plot of ΔT_m versus ϕ_1^2

where R is the gas constant, V_1 is the molar volume of the repeating unit for component 1, and T_m is the melt temperature of the blend. *Figure 14* shows a plot of the observed melting point depression of ETFE as a function of the square of the volume fraction of PMMA. At least-squares fit of the data yields a straight line intersecting the vertical axis near zero with a coefficient of regression of 0.97. Using the values $\rho_1 = 1.19\ g\ cm^{-3}$, $\rho_2 = 1.7\ g\ cm^{-3}$, $T_m^\circ = 240°C$, $V_1 = 84.0\ cm^3\ mol^{-1}$, $V_2 = 75.3\ cm^3\ mol^{-1}$ and $\Delta H_2 = 4.3\ kcal\ mol^{-1}$ ([29]), the calculated value of B is $-0.84\ cal\ cm^{-3}$. The calculated value of χ is -0.07 at 235°C. This absolute value of χ is considerably smaller than the one determined by Nishi and Wang[8] for the PMMA and PVF_2 system ($\chi = -0.298$ at 160°C). A small negative value of χ suggests that this system is miscible with very weak interactions in the molten state. However, it is important to point out that in the determination of χ we have not included the effect of morphology which can lead to an underestimation of χ as pointed out by Rims and Runt[33]. The heat of fusion of ETFE increases as the PMMA content increases, as shown in *Table 3*, suggesting that PMMA promotes crystallization of ETFE.

X-ray diffraction

Figure 15 shows the X-ray diffraction data of the pure polymers and their blends. The WAXD patterns of ETFE exhibit a single diffraction peak at $2\theta = 18.6°$, which is consistent with the literature[13–15]. For PMMA, the WAXD pattern gives a typical character of an amorphous polymer and there is only a broad diffusive background. The diffraction peak of ETFE of the blends stays invariant with blend composition, indicating that PMMA has no detectable effect on the crystal structure of ETFE.

CONCLUSIONS

(1) The ETFE/PMMA blends are semicompatible. The blends have three phases—a semicrystalline phase and two amorphous phases.

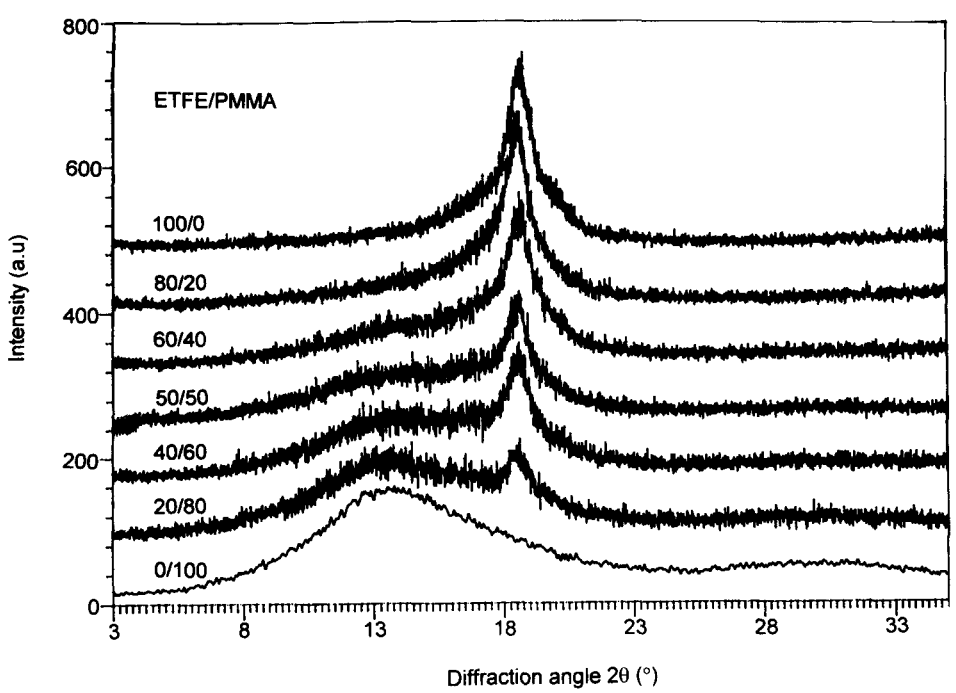

Figure 15 X-ray diffraction data for the ETFE/PMMA blends

(2) The interactions between ETFE and PMMA molecules are very weak.
(3) PMMA has no detectable effect on the crystal form of ETFE but the T_m and the crystallinity of ETFE decreases and increases, respectively, as the PMMA content increases.

ACKNOWLEDGEMENT

This work was supported by the Hong Kong Government Research Grant Council under the grant number HKUST 582/95P.

REFERENCES

1. Paul, D. R. and Newman, S., *Polymer Blends*, Vols. 1 and 2. Academic Press, New York, 1978.
2. Olabish, O., Robson, M. and Shaw, M. T., *Polymer–Polymer Miscibility*. Academic Press, New York, 1979.
3. Utracki, L. A., *Polymer Alloys and Blends*. Hanser Publishers, Munich, 1989.
4. Coleman, M. M., Graf, J. F. and Painter, P. C., *Specific Interaction and Miscibility of Polymer Blends*. Technomic Publishing, Lancaster, PA, 1991.
5. Grinsted, R. A. and Koenig, J. L., *Polym. Prepr.*, 1988, **29**, 15.
6. Telely, P., Laupretre, F. and Monnerie, L., *Polymer*, 1985, **26**, 1081.
7. Ward, T. C. and Lin, T. S., *Polym. Prepr.*, 1983, **24**, 136.
8. Nishi, T. and Wang, T. T., *Macromolecules*, 1975, **8**, 909.
9. Douglass, D. C. and McBriety, V. J., *Macromolecules*, 1978, **11**, 766.
10. Nishi, T. and Kobunshi, J., *Macromolecules*, 1977, **24**, 48.
11. Nishi, T. and Wang, T. T., *Macromolecules*, 1976, **9**, 603.
12. Hourston, D. J. and Hughes, I. D., *Polymer*, 1977, **18**, 1175.
13. Tanigami, T., Yamaruma, K., Ishikawa, M., Mizogachi, K. and Myasaka, K., *Polymer*, 1986, **27**, 999.
14. Tanigami, T., Yamaruma, K., Ishikawa, M., Mizogachi, K. and Myasaka, K., *Polymer*, 1986, **27**, 1521.
15. D'Aniello, C., De Rosa, C., Guerra, G., Petraccone, V., Corradini, P. and Ajroldi, G., *Polymer*, 1995, **36**, 967.
16. Hirata, Y. and Kotaka, T., *Polym. J.*, 1981, **13**, 273.
17. Léonard, V., Halary, J.L. and Monnerie, L., *Polymer*, 1985, **26**, 1507.
18. Wahrmund, D. C., Berstein, R. E., Barlow, J. W. and Paul, D. R., *Polym. Eng. Sci.*, 1978, **18**, 677.
19. Berstein, R. E., Paul, D. R. and Barlow, J. W., *Polym. Eng. Sci.*, 1978, **18**, 683.
20. Berstein, R. E., Wahmund, D. C., Barlow, J. W. and Paul, D. R., *Polym. Eng. Sci.*, 1978, **18**, 1220.
21. Paul, D. R., Barlow, J. W., Berstein, R. E. and Wahrmund, D. C., *Polym. Eng. Sci.*, 1978, **18**, 1225.
22. Jwei, T.K., Patterson, G. D. and Wang, T. T., *Macromolecules*, 1976, **9**, 780.
23. Penning, J. P. and St. John Manley, R., *Macromolecules*, 1996, **29**, 77.
24. Penning, J. P. and St. John Manley, R., *Macromolecules*, 1996, **29**, 84.
25. Starkweather, H. W. Jr., *J. Polym. Sci.*, 1973, **11**, 587.
26. Wilson, F. C. and Starkweather, H. H. Jr., *J. Polym. Sci.*, 1973, **11**, 587.
27. Chu, B. and Wu, C., *Macromolecules*, 1987, **20**, 93.
28. Wu, C., Buck, W. and Chu, B., *Macromolecules*, 1987, **20**, 93.
29. Dobreva, A., Nikolov, A. and Kostov, G., *Cryst. Res. Technol.*, 1992, **27**, 903.
30. Sauer, R. B., Avakian, P. and Starweather, H. W. Jr., *J. Polym. Sci., Polym. Phys.*, 1996, **34**, 517.
31. Weng, T. L., Smith, T., Feng, J. and Chan C.-M., paper in preparation.
32. Ahn, S. H., An, J. H., Lee, D. S. and Kim, S. C., *J. Polym. Sci. Polym. Phys.*, 1993, **31**, 1627.
33. Rims, P. and Runt, J. P., *Macromolecules*, 1984, **17**, 1520.